# Exciton dynamics in perturbed vibronic molecular aggregates

C. Brüning, J. Wehner, J. Hausner, M. Wenzel, and V. Engel
*Universität Würzburg, Institut für Physikalische und Theoretische Chemie, Am Hubland, Campus Nord, Emil-Fischer-Str. 42, 97074 Würzburg, Germany*

(Received 4 August 2015; accepted 27 October 2015; published online 17 November 2015)

A site specific perturbation of a photo-excited molecular aggregate can lead to a localization of excitonic energy. We investigate this localization dynamics for laser-prepared excited states. Changing the parameters of the electric field significantly influences the exciton localization which offers the possibility for a selective control of this process. This is demonstrated for aggregates possessing a single vibrational degree of freedom per monomer unit. It is shown that the effects identified for the molecular dimer can be generalized to larger aggregates with a high density of vibronic states.  [http://dx.doi.org/10.1063/1.4936127]

## I. INTRODUCTION

The transport of excitation energy (excitons) in aggregates of organic molecules is one of the most fundamental and most challenging problems of modern organic photovoltaics.[1–3] The reason is that, after being prepared by photo-absorption, the exciton has to travel over some spatial range to reach a boundary where it can be transformed into a charge separated state. Only then, free charges are generated which give rise to a photovoltaic current.

In an initial step, discarding any kind of disorder or other perturbations, photon absorption creates a de-localized electronically excited state in an aggregate $(M_1 - M_2 - \cdots - M_{N-1} - M_N)$ which can be viewed as a superposition of states corresponding to the excitation of a single monomer $M_n^*$ in the composed system. The coupling between the respective configurations $(M_1 - M_2 - \cdots - M_n^* - \cdots - M_N)$ leads to an energy transfer dynamics as, e.g., studied in Refs. 4 and 5. For an excellent review on vibronic dynamics in molecular aggregates, see Ref. 6. Regarding only next-neighbor couplings and taking symmetry into account, one does not expect, in the average, a substantial localization of the exciton on a smaller aggregate unit like, e.g., a monomer or a dimer. Suppose now that the interaction with an environment (solvent) results in a perturbation of the system. One might imagine that a finite time-dependent perturbation acts locally on a smaller part of the molecule which induces a disorder.[7–9] Then, symmetry is broken and the energy transfer is influenced. As predicted theoretically,[10] such processes might be characterized by two-dimensional optical spectroscopy.[11–15] In a former work, we showed that such interactions can lead to exciton localization, at least for the time the perturbation is effective.[16] If the localization remains stable for some time $\tau_l$, it is possible that an electronic relaxation process takes place subject to the condition that the relaxation time $\tau_r$ is shorter than $\tau_l$. This, for example, was observed in femtosecond experiments on perylene bisimide aggregates where the photo-excited state decays on a time-scale of about 200 fs.[17] Because such processes trap the exciton, it is highly desirable to avoid a localization maintained on a longer time-scale. In this paper, we present a model study where a time-dependent term is included in the excited state Hamiltonian to simulate an external perturbation in a simple way. It is then investigated how the nature of the initially prepared excited state determines the exciton localization. This is very much in the sense of "state-selective chemistry" which is one way to influence chemical reactions by preparation of a specific initial state.[18,19] In doing so, we hope to gain some insight into the possibility for a

 

quantum control of the localization and, in particular, to exclude it so that a more effective exciton diffusion may take place. The molecular dimer has been studied extensively as a model system for molecular aggregates.[6,20–25] Therefore, we start our work with an investigation of the dimer. Afterwards, the question will be addressed if the identified effects are transferable to larger systems. In Sec. II, we present the theory and the model. The results are contained in Sec. III which ends with a summary of the article.

## II. THEORY AND MODEL

We regard an aggregate consisting of $N$ monomers $M_n$. For each monomer, two electronic states $|g^M, n\rangle$ (ground state) and $|e^M, n\rangle$ (excited state) and a single vibrational degree-of-freedom ($x_n$) are taken into account. The Hamiltonian of monomer ($n$) is

$$\hat{H}^M(x_n) = |g^M, n\rangle\, H_g^M(x_n)\langle g^M, n| + |e^M, n\rangle\, H_e^M(x_n)\langle e^M, n|. \tag{1}$$

The vibrational Hamiltonians are

$$H_g^M(x_n) = -\frac{1}{2}\frac{\partial^2}{\partial x_n^2} + \frac{1}{2}\omega_0^2 x_n^2, \tag{2}$$

$$H_e^M(x_n) = -\frac{1}{2}\frac{\partial^2}{\partial x_n^2} + \frac{1}{2}\omega_0^2 (x_n - x_e)^2 + \Delta. \tag{3}$$

Thus, the vibrations are described by shifted harmonic oscillators (shift $x_e$ in the equilibrium distance) with equal frequency ($\omega_0$) in the ground and excited states, and an energy offset $\Delta$.

Denoting the vibrational coordinates collectively as $\vec{x} = (x_1, x_2, ..., x_N)$, the aggregate Hamiltonian is constructed from the monomer Hamiltonians as

$$\begin{aligned}\hat{H}^{(j)} = \hat{H}_g + \hat{H}_e = |g^A\rangle\, H_g(\vec{x})\langle g^A| + \sum_{n=1}^{N} |e,n\rangle\, H_{e,n}(\vec{x})\langle e,n| + \left(\sum_{n=1}^{N-1} |e,n\rangle\, J\, \langle e,n+1|\right) \\ + \left(\sum_{n=1}^{N-1} |e,n+1\rangle\, J\, \langle e,n|\right) + \left(|e,N\rangle\, J\, \langle e,1| + |e,1\rangle\, J\, \langle e,N|\right)\delta_{jc},\end{aligned} \tag{4}$$

where ($j$) is ($c$) for a cyclic and ($l$) for a linear aggregate geometry, respectively. The aggregate ground state is assumed as separable so that

$$H_g(\vec{x}) = \sum_{n=1}^{N} H_g^M(x_n), \quad |g^A\rangle = \prod_{n=1}^{N} |g^M, n\rangle. \tag{5}$$

The electronically excited states differ in the localization of the electronic excitation residing on the different monomers

$$H_{e,n}(\vec{x}) = H_e^M(x_n) + \sum_{(m\neq n)=1}^{N} H_g^M(x_m), \quad |e,n\rangle = |e^M, n\rangle \prod_{(m\neq n)=1}^{N} |g^M, m\rangle. \tag{6}$$

To describe the perturbation of the aggregate in a simple way, time-dependent terms as

$$\hat{W}_p(t) = \sum_{n_p} |e, n_p\rangle\, W(t)\, \langle e, n_p|, \tag{7}$$

with $W(t) = \lambda g(t)$, are added to the excited state Hamiltonian. Here, $\lambda$ is a parameter representing an energy shift, and the shape function $g(t)$ is

$$(t \le t_i): \; g(t) = e^{-\beta(t-t_i)^2}, \;\; (t_i \le t \le t_f): \; g(t) = 1, \;\; (t \ge t_f): \; g(t) = e^{-\beta(t-t_f)^2}. \tag{8}$$

Thus, the term $\hat{W}_p(t)$ introduces a temporal energy shift of the excited state Hamiltonians in selected monomers which are numbered by $n_p$. Such shifts can be caused by a single collision of a particle with the aggregate, and we aim at the characterization of these basic events. The introduction of the time-dependent term $\hat{W}_p(t)$ describes the respective interaction in a semi-classical way.[26] Despite the fact that this approximation is not energy-conserving, the system remains fully coherent.

The electronic excitation from the aggregate ground state becomes effective through the interaction with a laser pulse as

$$E(\omega, t) = f(t - t_0)\cos[\omega(t - t_0)], \tag{9}$$

with a Gaussian shape function $f(t - t_0)$ centered at time $t = t_0$ and the frequency $\omega$. The electric dipole interaction is

$$\hat{W}_\mu(t) = -E(\omega, t)\sum_n |e^M, n\rangle\, \mu_{eg}\, \langle g^M, n| + \text{h.c.}, \tag{10}$$

where $\mu_{eg}$ is the monomer transition dipole moment. We treat the special case that all transition dipole moments are parallel and constant so that the dipole coupling to all excited states $|e, n\rangle$ is identical.

We solve the time-dependent Schrödinger equation

$$i\frac{\partial}{\partial t}|\underline{\psi}(t)\rangle = \left[\hat{H}^{(j)} + \hat{W}_\mu(t) + \hat{W}_p(t)\right]|\underline{\psi}(t)\rangle, \tag{11}$$

in $N$ vibrational degrees-of-freedom for the $(N + 1)$ coupled components of the total wave function

$$\langle\vec{x}|\underline{\psi}(t)\rangle = \underline{\psi}(\vec{x}, t) = (\psi_g(\vec{x}, t), \; \psi_{e,1}(\vec{x}, t), \ldots, \psi_{e,N}(\vec{x}, t)). \tag{12}$$

For the time-propagation, the multiconfigurational time dependent Hartree method[27,28] is employed. Five single particle functions for each vibrational degree of freedom in each electronic state, represented in a basis of 13 harmonic oscillator functions, are used. The excited state wave functions are propagated within the constant mean field integration scheme keeping the integrator settings at the program's defaults. The time-step is chosen as 0.5 fs.

The parameters which determine the vibrational Hamiltonians are $\omega_0 = 0.175\,\text{eV}$, $x_e = 2.75\,\text{eV}^{-1}$, $\Delta = 2.35\,\text{eV}$, and the electronic coupling element is $J = 0.0175\,\text{eV}$. Similar values have been used in our studies on the optical properties of perylene bisimide aggregates where, within the model described above, absorption[5,29] and circular dichroism spectra[30] were calculated in excellent agreement with experiment.

Localization of an exciton on monomer $(n)$ in the aggregate is measured by the population in state $|e, n\rangle$ defined as

$$P_n(t) = \int d\vec{x}\, |\psi_{e,n}(\vec{x}, t)|^2. \tag{13}$$

## III. RESULTS

We start with the simplest aggregate, the molecular dimer $(N = 2)$. In our former study,[16] it was shown that, if the vibronic ground state $\psi_{00}(x_1, x_2)$ (with energy $E_{00}$) is placed in the excited states ($\delta$-pulse excitation or impulsive limit[31]), i.e., $\psi_{e,m}(x_1, x_2, 0) = \mu_{eg}\psi_{00}(x_1, x_2)$, the perturbation always leads to a localization in the state $|e, m\rangle$ with higher energy. This is illustrated in Fig. 1. The time-dependent perturbation $\hat{W}_p(t)$, here acting on monomer $n_p = 1$, is also shown in the figure, where the strength has a value of $\lambda = 0.16\,\text{eV}$. This number is about a factor of ten larger than the coupling constant $J$. As was shown before,[16] the localization effects described below are of the

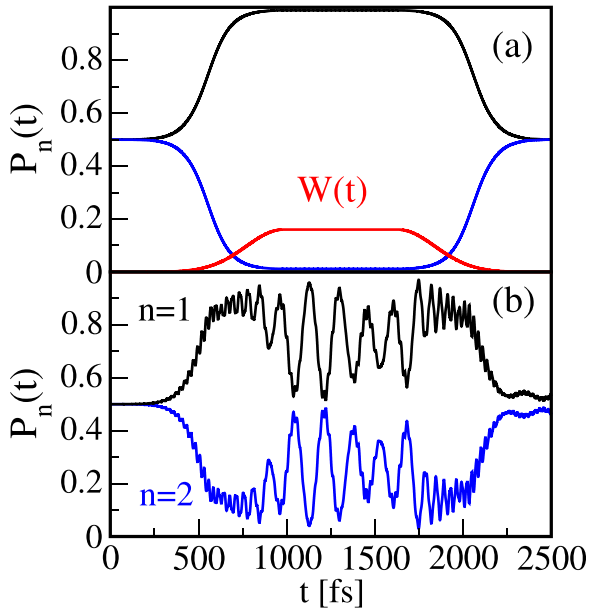


FIG. 1. Dimer populations $P_n(t)$ calculated for transitions out of the vibronic ground state in the impulsive limit. The upper panel shows the curves obtained for a system of two coupled excited state levels. The corresponding curves where the Hamiltonian includes vibrational modes are displayed in the lower panel. Also shown is the time-dependent perturbation $W(t)$ which produces an energy shift of the Hamiltonian of monomer $n_p = 1$.

same magnitude if the ratio $J/\lambda$ is varied over a reasonable range, so that here we do not present calculations for other values of the parameters. The value of $\lambda = 0.16\,\text{eV}$ is chosen to include the possibility of population transfer between shifted vibrational levels, see below. Panel (a) contains the case of a coupled two-level system, i.e., where the excited state Hamiltonians $H_{e,n}$ are replaced by numbers $E$. It is seen that the perturbation results in a complete localization in the perturbed state $|e,1\rangle$. Taking vibrations into account leads to the curves displayed in panel (b) of Fig. 1. A similar behavior as seen in the two-level system is encountered, but additional oscillations of the populations occur during the time the perturbation is effective. They can be explained by a near-resonant transfer between vibrational levels of the unperturbed ($|e,2\rangle$) and perturbed states ($|e,1\rangle$), and they disappear for smaller values of $\lambda$ leading to an identical dynamics as seen in the purely electronic case. On the other hand, if the energy shift $\lambda$ is set equal to the vibrational quantum $\omega_0$, a complete exchange of population between the two states takes place, for an extended discussion see Ref. 16. Depending on how the perturbation is switched off, oscillations with smaller or larger amplitudes remain at longer times.

Abandoning the impulsive limit, we next take laser-pulse excitation into account. In Fig. 2, lower panel, the absorption spectrum for the dimer is displayed within a selected energy interval. It is calculated as[32,33]

$$\sigma_{00}(\omega) = \int dt\, e^{i\omega t}\, \langle \underline{\psi}_e(0) | \hat{U}_e(t) | \underline{\psi}_e(0) \rangle, \tag{14}$$

where $\hat{U}_e(t)$ is the propagator containing the excited state part $\hat{H}_e$ of the total Hamiltonian $\hat{H}^{(l)}$ (Eq. (4)), and the initial condition is $\psi_{e,m}(x_1,x_2,0) = \mu_{eg}\psi_{00}(x_1,x_2)$. For the weak coupling and the chosen parallel dipole geometry, the spectrum has a simple shape[22,34] showing bands separated by the vibrational quantum $\omega_0$. From the peak positions, we determine the excited state eigenenergies $E^\alpha$ and calculate wave functions $(\psi^{(\alpha)}_{e,1}(x_1,x_2), \psi^{(\alpha)}_{e,2}(x_1,x_2))$ employing pulses with photon energies which match the energy differences to the vibronic ground state. The field strengths are chosen such that first-order time-dependent perturbation theory applies. We do not provide the numbers for the field strengths, being different for the different aggregate sizes. These parameters are not relevant because after the laser-excitation, the respective eigenfunctions are normalized, and no further interaction with the ground electronic state occurs.

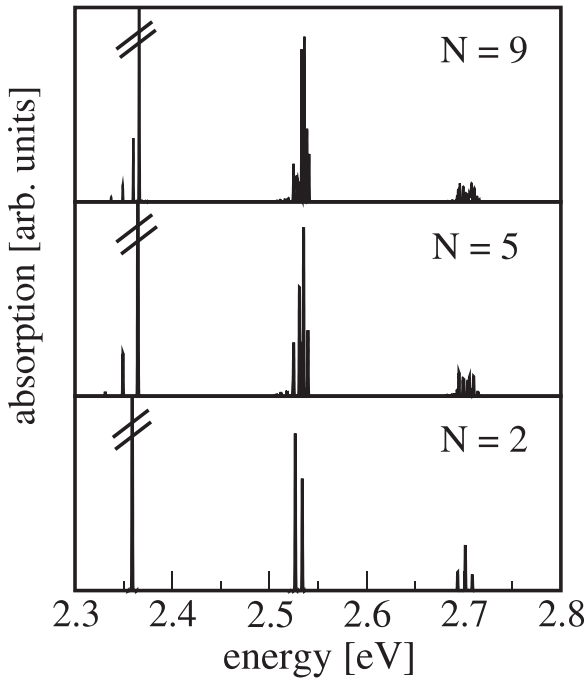


FIG. 2. Absorption spectra for linear aggregates with $N=2$ (dimer), $N=5$ (pentamer), and $N=9$ (nonamer). The peaks with the highest intensities are truncated in each case.

We use Gaussian pulses with a spectral width of 5 meV, so that only a single eigenstate is excited in each case. The real part of the normalized eigenfunctions corresponding to the six peaks seen in the dimer spectrum (Fig. 2) is displayed in Fig. 3. Because the initial state is the vibronic ground state which is symmetric with respect to the exchange of the two monomers and the monomer transition dipole moments are at an angle of $\gamma=0$, absorption takes place into the (+)-band of the spectrum[35] which corresponds to symmetric final states. This means that $\psi^{(\alpha)}_{e,1}(x_1,x_2)=\psi^{(\alpha)}_{e,2}(x_2,x_1)$, as can be verified by inspection of Fig. 3.

In Fig. 4, we show the population dynamics for times after the pulse excitation, where panels (a)–(f) correspond to the initially populated excited state eigenfunctions depicted in Fig. 3, panels (a)–(f). In each case, the perturbation applied to the monomer ($n_p=1$) Hamiltonian (with $\lambda=0.16$ eV) causes a transient localization. Several trends can be observed. First, the curves in panels (a), (c), (f) and (b), (e) are the same, respectively. The curve in panel (d) differ from all others because localization is found in the unperturbed state. To get an insight into the dynamics of the perturbed system, we regard the short-time dynamics, expanding the time-evolution operator to second order in the time-step $dt$

$$|\underline{\psi}_e(dt)\rangle \approx \left[1-idt\left(\hat{H}_e+\hat{W}_p(dt)\right)-\frac{dt^2}{2}\left(\left(\hat{H}_e+\hat{W}(dt)\right)^2\right)\right]|\underline{\psi}^{(\alpha)}_e(0)\rangle. \tag{15}$$

Ignoring the shape function $g(t)$ by setting the perturbation to the constant value $W(dt)=\lambda$, the two components of the excited state wave function evolve as

$$\begin{pmatrix}\psi_{e,1}(dt)\\ \psi_{e,2}(dt)\end{pmatrix} \approx \begin{pmatrix}\psi^{(\alpha)}_{e,1}(0)\\ \psi^{(\alpha)}_{e,2}(0)\end{pmatrix} - idt\left[E_\alpha\begin{pmatrix}\psi^{(\alpha)}_{e,1}(0)\\ \psi^{(\alpha)}_{e,2}(0)\end{pmatrix}+\begin{pmatrix}\lambda\psi^{(\alpha)}_{e,1}(0)\\ 0\end{pmatrix}\right] - \frac{dt^2}{2}\left[E^2_\alpha\begin{pmatrix}\psi^{(\alpha)}_{e,1}(0)\\ \psi^{(\alpha)}_{e,2}(0)\end{pmatrix}+\begin{pmatrix}\lambda H_{e,1}\psi^{(\alpha)}_{e,1}(0)\\ \lambda J\psi^{(\alpha)}_{e,1}(0)\end{pmatrix}+E_\alpha\begin{pmatrix}\lambda\psi^{(\alpha)}_{e,1}(0)\\ 0\end{pmatrix}+\begin{pmatrix}\lambda^2\psi^{(\alpha)}_{e,1}(0)\\ 0\end{pmatrix}\right]. \tag{16}$$

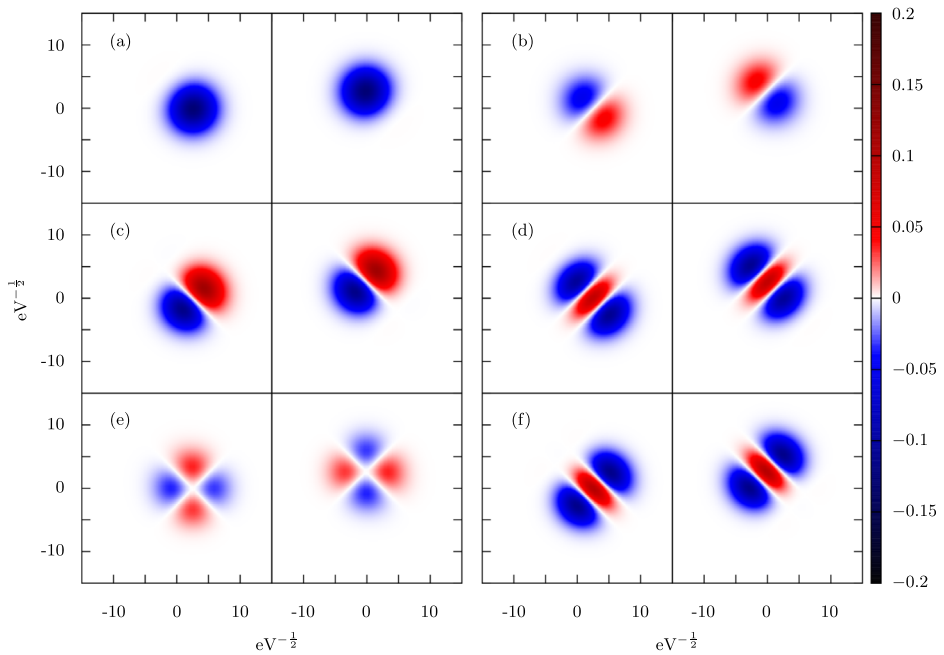


FIG. 3. Real part of the excited state eigenfunctions corresponding to energies $E_\alpha$ of 2.3589 eV (panel (a)), 2.5267 eV (panel (b)), 2.5339 eV (panel (c)), 2.6939 eV (panel (d)), 2.7018 eV (panel (e)), and 2.7090 eV (panel (f)), respectively. Shown are the two components $\psi^{(\alpha)}_{e,1}(x_1, x_2)$ (left sides) and $\psi^{(\alpha)}_{e,2}(x_1, x_2)$ (right sides).

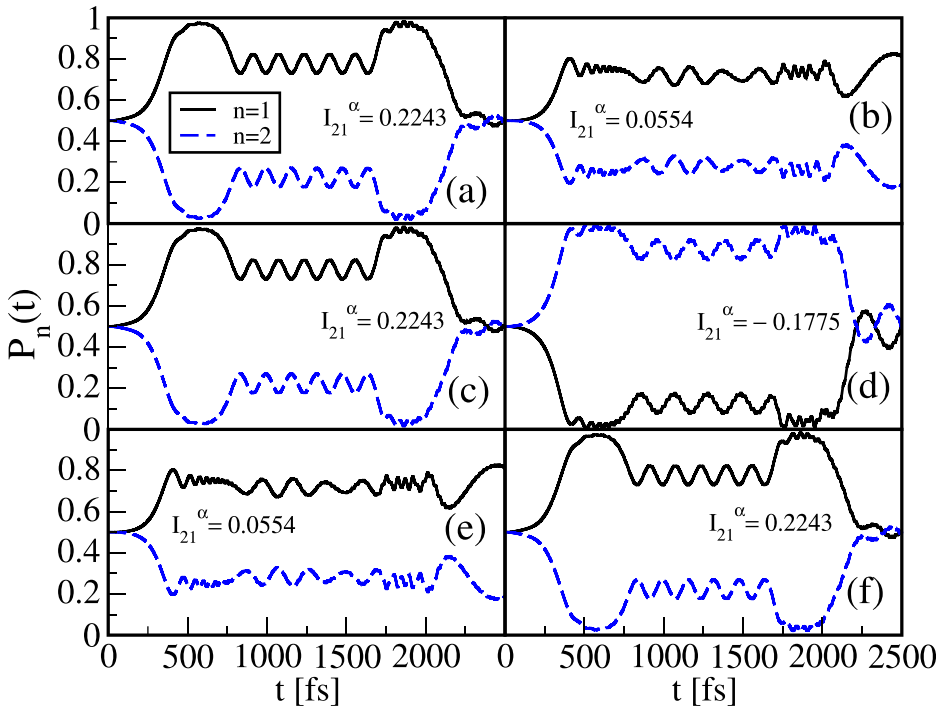


FIG. 4. Dimer populations $P_n(t)$ calculated for the initially populated eigenfunctions displayed in Fig. 3. The values of the overlap integrals $I^{\alpha}_{nm}$ (Eq. (18)) are included in each case.

The population $P_2(dt)$ is now determined in the order $dt^2$ and as

$$P_2(dt) \approx P_2(0) - I_{21}^{\alpha}\, \lambda J\, dt^2, \tag{17}$$

with the definition of the (real valued) overlap integral

$$I_{21}^{\alpha} = \langle \psi_{e,2}^{(\alpha)}(0) | \psi_{e,1}^{(\alpha)}(0) \rangle. \tag{18}$$

Thus, for short times and positive values of $\lambda$ and $J$ (as in our example), the population in the unperturbed state decreases or increases depending on the sign of the overlap $I_{21}^{\alpha}$. Concerning the numerical results shown in Fig. 4, these overlaps are positive with the exception of the case depicted in panel (d), see the numbers in the different panels. It then follows that the population in the unperturbed component (case (d)) increases upon the perturbation, whereas in all other situations, a decrease is to be expected. The numerical results confirm this prediction which is obviously also valid, at least in the average, for later times. Furthermore, in cases (b) and (e), the smaller value of $I_{\alpha}$ leads to a less pronounced localization if compared to the situations in panels (a), (c), and (f). We have analyzed the integrands in the overlap integrals Eq. (18) and found that they are purely positive in the latter cases and show zero, one and two nodes along the diagonal $x_1 = x_2$, respectively, which then leads to a relatively large (and identical) value of the integral. On the other hand, for cases (b) and (e), the integrands contain positive and negative parts with the latter covering a less extended area. This, upon integration, leads to smaller but still positive values of $I_{21}^{\alpha}$. Finally, for the exception (panel (d)), the negative areas dominate so that the overlap integral has a negative value.

As documented above, the localization depends on the initial excited state eigenfunction of the system. In particular, excitation at a photon energy of 2.6939 eV (Figs. 3 and 4, panel (d)) leads to the opposite behavior as found for the neighbor states with eigenenergies of 2.7018 eV (Figs. 3 and 4, panel (e)) and 2.7090 eV (Figs. 3 and 4, panel (f)), respectively. This suggests that the preparation of a wave-packet consisting of a superposition of these three states could lead to a reduced degree of localization. Indeed, using a pulse at an energy of 2.6939 eV and a spectral width of 0.0268 eV yields a situation where, as long as the perturbation interacts, the population remains nearly constant, as is documented in Fig. 5. Thus, a variation of the photon energy and the pulse-width allows for a quantum control of the population dynamics when the external perturbation is active so that localization can be enforced on one or the other dimer configuration or even be suppressed. We note that if the laser-field is not switched off and excitation proceeds, the dynamics remains almost unchanged. In that case additional oscillations are seen which are associated with the energy shifting of the dimer spectrum so that the field is no longer resonant with a transition in the unperturbed system (not shown).

Next, larger aggregates are treated to investigate if the dimer results can be transferred to more extended systems. As an example, a nonamer in a cyclic and also a linear arrangement is treated. The model Hamiltonian has nine vibrational degrees of freedom and nine coupled excited states, which leads to a high density of states. This can be anticipated from the low energy part of the absorption spectrum shown in Fig. 2, upper panel. Figure 6 shows the population dynamics for the unperturbed case in panels (a) (linear) and (d) (cyclic), respectively. The initial wave function obtained by a $\delta$-pulse excitation has equal components ($\psi_{e,m} = \mu_{eg}\psi_{00}$) so that we start from a completely de-localized state. It is seen that, for the linear aggregate, the population tends to temporarily accumulate in the middle of the aggregate (monomer $n_p = 5$). For the cyclic arrangement, due to the initial complete delocalization and the cyclic boundary condition, no population dynamics takes place.

Results for the case of the weaker perturbation ($\lambda = 0.0175$ eV, this is in the range of the thermal energy of a particle colliding with the aggregate at room temperature) which acts on monomer $n_p = 3$ are shown in panels (b) and (e) of Fig. 6 for the linear and cyclic geometry, respectively. As in the dimer case, localization is found in the disturbed state for both aggregate geometries. This changes if a resonant perturbation ($\lambda = \omega_0$) is applied (panels (c) and (f)). Because of

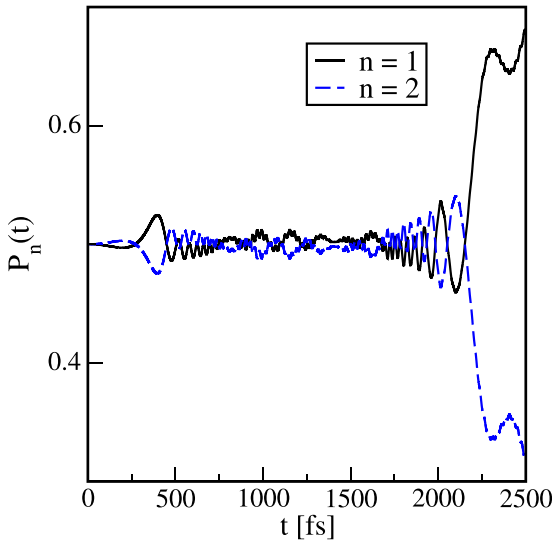


FIG. 5. Population dynamics starting from an initial state wave packet which is a superposition of excited state eigenfunctions with eigenenergies corresponding to the peaks present in the dimer absorption spectrum around an energy of 2.7 eV (Fig. 2).

resonant coupling between different vibrational levels, the population which initially accumulates in the perturbed state moves through the aggregate so that a de-localized situation is encountered. Thus, the effects which have been identified for the dimer are also present in the nonamer. The same applies to smaller aggregates ($N = 3$–8) which was checked upon numerically (not shown).

We now address the question what happens if the perturbation acts on several monomer sites. Therefore, the interaction $\hat{W}_p(t)$ is applied to the monomers $n_p = 3$ and $n_p = 4$ in the nonamer. In Fig. 7, we compare populations for the linear and cyclic arrangement and for a weak ($\lambda = 0.0175$ eV) and the resonant ($\lambda = \omega_0$) interaction. A similar behavior as discussed above (single monomer excitation) is found. For the weak interaction (panels (a) and (c)), mainly the perturbed states are populated and out-of-phase oscillations between these states are seen in the linear case, whereas for the cyclic arrangements in phase oscillations of $P_3(t)$ and $P_4(t)$ are found. As before, if the coupling strength $\lambda$ is increased towards resonance and the perturbation remains constant, the population moves through the entire aggregate (panels (b) and (d)). We

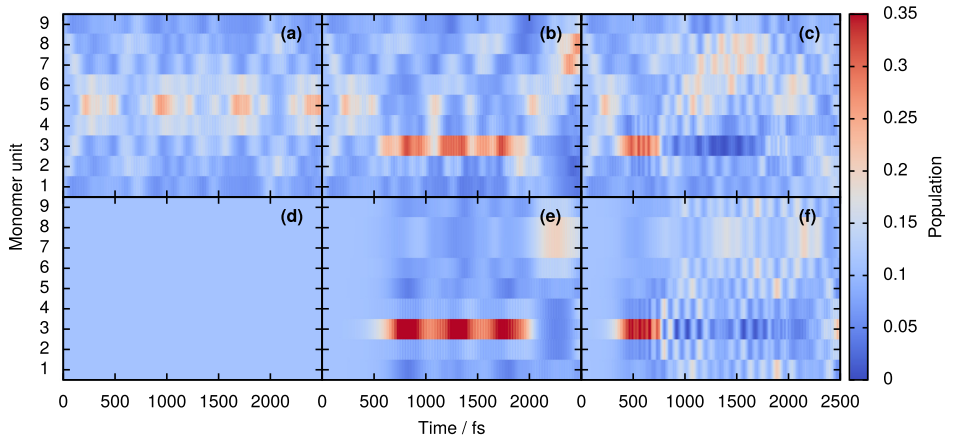


FIG. 6. Population dynamics in the nonamer. Initially, all states $|e, n\rangle$ are populated equally. Panels (a) and (d) illustrate the non-perturbed case for the linear and cyclic geometry, respectively. Including a weak and resonant coupling on monomer $n_p = 3$ leads to the dynamics displayed in panels (b) and (c) (linear) and (e) and (f) (cyclic).

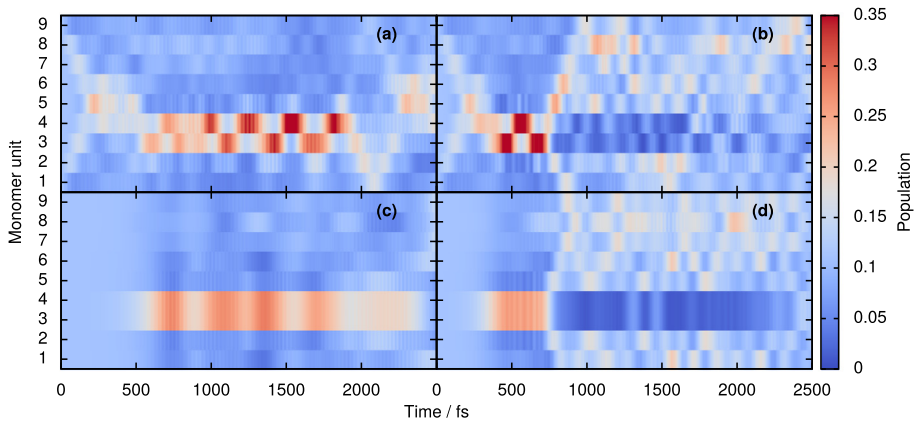


FIG. 7. Population dynamics in the nonamer. Initially, all states $|e,n\rangle$ are populated equally but here the perturbation acts on monomers $n_p = 3$ and 4. The upper/lower panels correspond to the linear/cyclic configuration with weak (panel (a) and panel(c)) and resonant (panel (b) and panel (d)) perturbation.

thus conclude that even for a perturbation interacting over a larger spatial region, the trends inferred from the dimer are valid.

Next, we treat the situation, where different eigenstates are prepared by a laser excitation before the perturbation sets in. Because of the high density of states in the nonamer, we regard the case of a linear pentamer ($N = 5$). We concentrate on the first absorption band seen in Fig. 2 at energies around 2.35 eV which corresponds to the case where no vibrational excitation is present so that the vibrational wave functions in all components are node-less. To get an insight into the transfer dynamics, it is then sufficient to perform an analytical calculation for the pure electronic system. Note, however, that the numerical results presented in Fig. 8 derive from the full vibronic pentamer system. Replacing the complete vibronic problem for the excited state by a

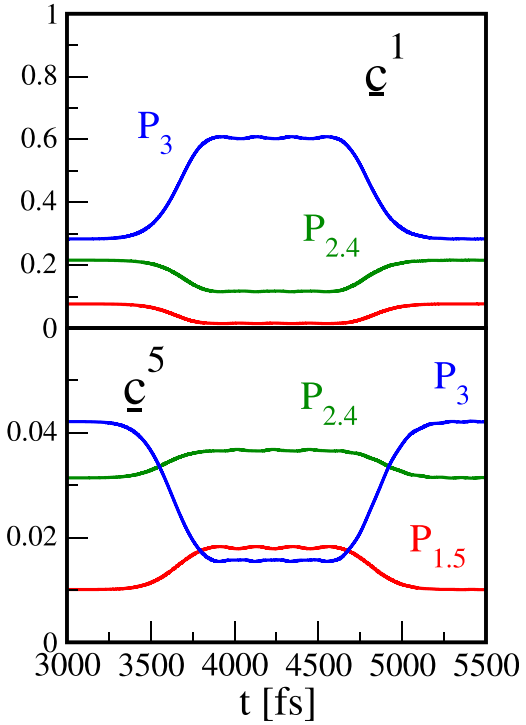


FIG. 8. Population dynamics in the pentamer. Initially, different eigenstates (characterized by their electronic coefficient vectors $\underline{c}^k$, (Eq. (20)) are prepared through selective laser excitation. The perturbation acts on monomer $n_p = 3$.

coupled degenerate 5-level system, the eigenenergies and -vectors can be calculated analytically.[36] For the $(n)$-component of eigenvector $(k)$, one finds

$$c_n^k = \frac{1}{\sqrt{3}} \sin\left(\frac{nk\pi}{6}\right). \tag{19}$$

In the regarded dipole-geometry, transitions are only allowed to final states with $(+)$-parity. As an example, we consider the eigenvectors $(a = \sqrt{3}/2)$

$$\underline{c}^1 = \frac{1}{\sqrt{3}}(0.5, a, 1, a, 0.5), \quad \underline{c}^5 = \frac{1}{\sqrt{3}}(0.5, -a, 1, -a, 0.5). \tag{20}$$

Since the vibrational wave functions are node-less, it follows that the signs appearing in the different components of the electronic eigenvectors determine the overlap integrals $I_{nm}^{\alpha}$ which are important for the population transfer dynamics, see Eq. (18). Adding the perturbation $(\lambda = 0.0175\,\text{eV})$ to the excited state of the middle monomer $(n_p = 3)$, leads to the dynamics shown in Fig. 8. The upper panel corresponds to the initial eigenstate with electronic coefficient $\underline{c}^1$ (at an energy of 2.365 eV in the pentamer spectrum), whereas the lower panel shows the case for $\underline{c}^5$ (2.350 eV). Following the same reasoning as applied to the dimer, we have to regard the overlap integral between the component of the perturbed state $|3, e\rangle$ and the next-neighbor components. From the coefficients given in Eq. (20), one then predicts an equal decrease of the population $P_2(t)$ and $P_4(t)$ in the case $k = 1$ (positive overlap integral) and an increase in case $k = 5$ (negative overlap integral). This indeed is the case as can be taken from Fig. 8.

Until now, the perturbation $\hat{W}_p(t)$ consists of a smoothly varying function of time. In order to account for different scattering events occurring in a molecular sample, we return to the dimer system and modify the perturbation to include fluctuations. The latter derive from a function $f_n = f(\omega_n)$ in frequency space, which decays proportional to $\omega_n^{-1.25}$. Different realizations are obtained in modifying each value $f_n$ with a random phase taken from the half-open interval $[0,2\pi)$ and Fourier transforming the obtained function to time-domain. Thus, the constructed fluctuations are scaled so that their maximum is $\lambda/4$. Four realizations of such fluctuations are displayed in the lower panel of Fig. 9 $(\lambda = 0.0175\,\text{eV})$. It is expected that an average over many realizations of the fluctuating term results in a certain degree of de-coherence. That this is indeed the case illustrated in regarding the averaged electronic density matrix element

$$C_{12}(t) = \frac{1}{N_f} \sum_{l=1}^{N_f} \langle \psi_{e,1,l}(t) | \psi_{e,2,l}(t) \rangle, \tag{21}$$

where $N_f$ is the number of realizations, each leading to vibrational wave functions $\psi_{e,j,l}(x_1, x_2, t)$. In Fig. 9, middle panel, we show the absolute value $|C_{12}(t)|$ obtained for $N_f = 100$. It is seen that the perturbations lead to an average decrease of the oscillation amplitude which goes in hand with a loss of coherence. However, comparing the populations $P_n^a(t)$ obtained by an average over all realizations (upper panel of the figure) with the noise-free case $(P_n(t))$, it is found that the localization dynamics is nearly unchanged at times when the perturbation is non-zero. As an important result, we note that including bath-fluctuations does not change the results obtained for the cases where no noise is present—at least in the parameter range regarded here.

To conclude, we present a study on the population dynamics in molecular aggregates under perturbation. The latter is chosen in a simple form and consists of a shift of the excited state Hamiltonian for one or more monomers within the aggregate. Starting from a delocalized excited state, the perturbation results in a localization of population and thus excitonic energy on certain monomer sites. Regarding first the molecular dimer, it is shown that this effect is state selective: the laser-preparation of different excited state eigenfunctions is followed by a different localization dynamics. In particular, by selectively choosing a particular initial state, it

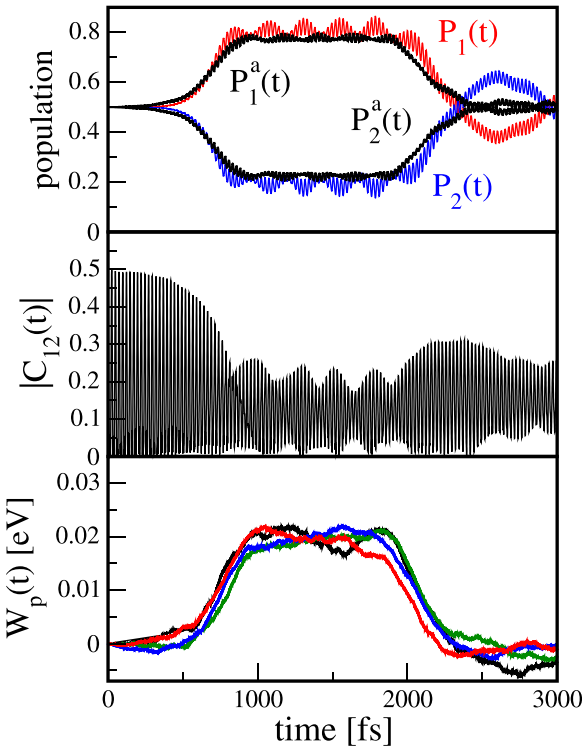


FIG. 9. Localization dynamics in the dimer system under the influence of noise. Upper panel: comparison of the noise-free case ($P_n(t)$) with the case including fluctuations ($P_n^a(t)$), where in the latter case an average over 100 realizations is performed. Middle panel: absolute value of the averaged electronic density matrix element $|C_{12}(t)|$ as defined in Eq. (21). Lower panel: four single realizations of the noisy perturbation function.

is possible to steer the localization site selectively. The preparation of an excited state wave packet makes it furthermore possible to annihilate the perturbation-induced localization. Remarkably, effects which are identified for the dimer are as well present in more extended aggregates having much higher densities of states. This applies to the localization dynamics in general and also to its state-selectivity.

We have modified the time-dependent perturbation $\hat{W}_p(t)$ to include fluctuations by modulating it with different levels of random noise. It is found that the population dynamics is modulated by the noise but the general trends are the same as if fluctuations are excluded. Insofar, we are confident that the established results are also valid for a more general time-dependence of the perturbation.

## ACKNOWLEDGMENTS

Financial support within the FOR 1809 was gratefully acknowledged. This publication was funded by the German Research Foundation (DFG) and the University of Würzburg in the funding programme Open Access Publishing.

[1]J.-L. Brédas, D. Beljonne, V. Coropceanu, and J. Cornil, "Charge-transfer and energy-transfer processes in π-conjugated oligomers and polymers: A molecular picture," Chem. Rev. **104**, 4971–5003 (2004).
[2]M. R. Wasielewski, "Self-assembly strategies for integrating light harvesting and charge separation in artificial photosynthetic systems," Acc. Chem. Res. **42**, 1910 (2009).
[3]F. Würthner and K. Meerholz, "Systems chemistry approach in organic photovoltaic," Chem. Eur. J. **16**, 9366–9373 (2010).
[4]J. Roden, G. Schulz, A. Eisfeld, and J. S. Briggs, "Energy transfer on a vibronically-coupled quantum aggregate," J. Chem. Phys. **131**, 044909 (2009).
[5]J. Seibt, T. Winkler, K. Renziehausen, V. Dehm, F. Würthner, and V. Engel, "Vibronic transitions and quantum dynamics in molecular oligomers: A theoretical analysis with an application to aggregates of perylene bisimides," J. Phys. Chem. A **113**, 13475–13482 (2009).

[6]M. Schröter, S. D. Ivanov, J. Schulze, S. P. Polyutov, Y. Yani, T. Pullerits, and O. Kühn, "Exciton-vibrational coupling in the dynamics and spectroscopy of Frenkel excitons in molecular aggregates," Phys. Rep. **567**, 1–78 (2015).
[7]V. A. Malyshev, A. Rodriguez, and F. Dominguez-Adame, "Linear optical properties of one-dimensional Frenkel exciton systems with intersite energy correlations," Phys. Rev. B **60**, 14140 (1999).
[8]M. Bednarz, V. A. Malyshev, and J. Knoester, "Temperature dependent fluorescence in disordered Frenkel chains: Interplay of equilibration and local band-edge level structure," Phys. Rev. Lett. **91**, 217401 (2003).
[9]M. Bednarz, V. A. Malyshev, and J. Knoester, "Low-temperature dynamics of weakly localized frenkel excitons in disordered linear chains," J. Chem. Phys. **120**, 3827–3840 (2004).
[10]A. G. Dijkstra, T. la Cour Jansen, and J. Knoester, "Localization and coherent dynamics of excitons in the two-dimensional optical spectrum of molecular J-aggregates," J. Chem. Phys. **128**, 164511 (2008).
[11]J. D. Hybl, A. W. Albrecht, S. M. Gallagher Faeder, and D. M. Jonas, "Two dimensional electronic spectroscopy," Chem. Phys. Lett. **297**, 307 (1998).
[12]P. Tian, D. Keusters, Y. Suzaki, and W. S. Warren, "Femtosecond phase-coherent two-dimensional spectroscopy," Science **300**, 1553–1555 (2003).
[13]M. L. Cowan, J. P. Ogilvie, and R. J. D. Miller, "Two-dimensional spectroscopy using diffractive optics based phased-locked photon echoes," Chem. Phys. Lett. **386**, 184–189 (2004).
[14]T. Brixner, T. Mančal, I. V. Stiopkin, and G. R. Fleming, "Phase-stabilized two-dimensional electronic spectroscopy," J. Chem. Phys. **121**, 4221–4236 (2004).
[15]T. Brixner, J. Stenger, H. M. Vaswani, M. Cho, R. E. Blankenship, and G. R. Fleming, "Two-dimensional spectroscopy of electronic couplings in photosynthesis," Nature **434**, 625 (2005).
[16]J. Wehner, A. Schubert, and V. Engel, "Vibronic energy localization in weakly coupled small molecular aggregates," Chem. Phys. Lett. **541**, 49 (2012).
[17]A. Schubert, M. Falge, M. Kess, V. Settels, S. Lochbrunner, W. T. Strunz, F. Würthner, B. Engels, and V. Engel, "Theoretical analysis of the relaxation dynamics in perylene bisimide dimers excited by femtosecond laser pulses," J. Phys. Chem. A **118**, 1403 (2014).
[18]A. H. Zewail, "State-selective chemistry—Is it possible?," Phys. Today **33**(11), 27 (1980).
[19]F. F. Crim, "Vibrationally mediated photodissociation: Exploring excited-state surfaces and controlling decomposition pathways," Ann. Rev. Phys. Chem. **44**, 397–428 (1993).
[20]O. Sinanoglu, in *Modern Quantum Chemistry III*, edited by Th. Förster (Academic Press, New York, 1965), pp. 93–137.
[21]M. Kasha, H. R. Rawls, and M. A. El-Bayoumi, "Exciton model in molecular spectroscopy," Pure Appl. Chem. **11**, 371 (1995).
[22]R. L. Fulton and M. Gouterman, "Vibronic coupling II. spectra of dimers," J. Chem. Phys. **41**, 2280–2286 (1964).
[23]W. West and S. Pearce, "The dimeric state of cyanine dyes," J. Phys. Chem. **69**, 1894–1903 (1965).
[24]B. Kopainsky, J. K. Hallermeier, and W. Kaiser, "The first step if aggregation of pic: the dimerization," Chem. Phys. Lett. **83**, 498–502 (1981).
[25]A. Eisfeld, L. Braun, W. T. Strunz, J. S. Briggs, J. Beck, and V. Engel, "Vibronic energies and spectra of molecular dimers," J. Chem. Phys. **122**, 134103 (2005).
[26]J. S. Briggs and J. M. Rost, "Time-dependence in quantum mechanics," Euro. Phys. J. D **10**, 311–318 (2000).
[27]M. H. Beck, A. Jäckle, G. A. Worth, and H.-D. Meyer, "The multiconfiguration time-dependent Hartree method: A highly efficient algorithm for propagating wavepackets," Phys. Rep. **324**, 1–105 (2000).
[28]G. A. Worth, M. H. Beck, A. Jäckle, and H.-D. Meyer, The MCTDH Package, Version 8.2 (2000); H.-D. Meyer, Version 8.3 (2002), Version 8.4 (2007), see http://www.pci.uni-heidelberg.de/tc/usr/mctdh/.
[29]J. Seibt, P. Marquetand, V. Engel, Z. Chen, V. Dehm, and F. Würthner, "On the geometry dependence of molecular dimer spectra with an application to aggregates of perylene bisimide," Chem. Phys. **328**, 354 (2006).
[30]J. Seibt, V. Dehm, F. Würthner, and V. Engel, "Circular dichroism spectroscopy of small molecular aggregates: Dynamical features and size effects," J. Chem. Phys. **128**, 204303 (2008).
[31]W. Domcke and G. Stock, "Theory of ultrafast nonadiabatic excited-state processes and their spectroscopic detection in real time," Adv. Chem. Phys. **100**, 1 (1997).
[32]E. J. Heller, "The semiclassical way to molecular spectroscopy," Acc. Chem. Res. **14**, 368–375 (1981).
[33]R. Schinke, *Photodissociation Dynamics* (Cambridge University Press, Cambridge, 1993).
[34]C. Brüning, K. Renziehausen, and V. Engel, "On the parameterization of vibronic Hamiltonians for molecular aggregates using absorption line-shapes as an input," J. Chem. Phys. **139**, 054303 (2013).
[35]R. L. Fulton and M. Gouterman, "Vibronic coupling I. mathematical treatment for two electronic states," J. Chem. Phys. **35**, 1059–1071 (1961).
[36]V. May and O. Kühn, *Charge and Energy Transfer Dynamics in Molecular Systems*, 3rd ed. (Wiley-VCH, Weinheim, 2011).